

Accepted Manuscript

3,5-Diaryl-1*H*-pyrazolo[3,4-*b*]pyridines as potent tubulin polymerization inhibitors:
Rational design, synthesis and biological evaluation

Min'an Zhai, Shiyuan Liu, Meiqi Gao, Long Wang, Jun Sun, Jianan Du, Qi Guan, Kai Bao, Daiying Zuo, Yingliang Wu, Weige Zhang



PII: S0223-5234(18)31096-1

DOI: <https://doi.org/10.1016/j.ejmech.2018.12.053>

Reference: EJMECH 10987

To appear in: *European Journal of Medicinal Chemistry*

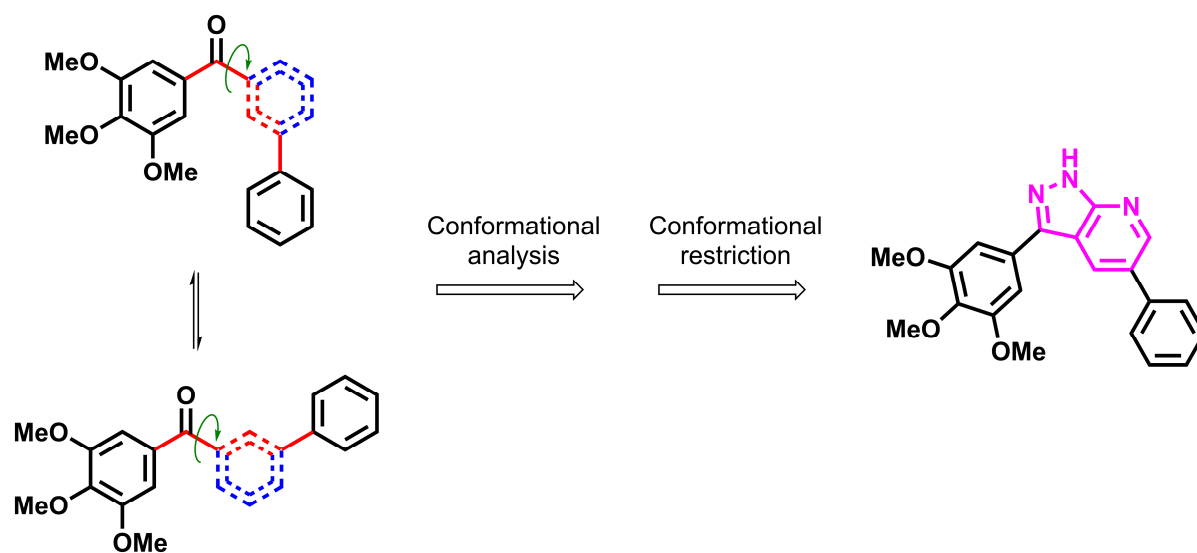
Received Date: 27 September 2018

Revised Date: 10 December 2018

Accepted Date: 21 December 2018

Please cite this article as: Min'. Zhai, S. Liu, M. Gao, L. Wang, J. Sun, J. Du, Q. Guan, K. Bao, D. Zuo, Y. Wu, W. Zhang, 3,5-Diaryl-1*H*-pyrazolo[3,4-*b*]pyridines as potent tubulin polymerization inhibitors: Rational design, synthesis and biological evaluation, *European Journal of Medicinal Chemistry* (2019), doi: <https://doi.org/10.1016/j.ejmech.2018.12.053>.

This is a PDF file of an unedited manuscript that has been accepted for publication. As a service to our customers we are providing this early version of the manuscript. The manuscript will undergo copyediting, typesetting, and review of the resulting proof before it is published in its final form. Please note that during the production process errors may be discovered which could affect the content, and all legal disclaimers that apply to the journal pertain.



ACCEPTED MANUSCRIPT

3,5-Diaryl-1*H*-pyrazolo[3,4-*b*]pyridines as potent tubulin polymerization inhibitors: Rational design, synthesis and biological evaluation

Min'an Zhai^a, Shiyuan Liu^a, Meiqi Gao^b, Long Wang^a, Jun Sun^d, Jianan Du^b, Qi Guan^{a*}, Kai Bao^c, Daiying Zuo^b, Yingliang Wu^{b*}, Weige Zhang^{a*}

^a Key Laboratory of Structure-Based Drug Design and Discovery, Ministry of Education, Shenyang Pharmaceutical University, 103 Wenhua Road, Shenhe District, Shenyang 110016, China

^b Department of Pharmacology, Shenyang Pharmaceutical University, 103 Wenhua Road, Shenhe District, Shenyang 110016, China

^c Wuya College of Innovation, Shenyang Pharmaceutical University, 103 Wenhua Road, Shenhe District, Shenyang 110016, China

^d Clinical Pharmacology Laboratory, Henan Province People's Hospital, 7 Weiwu Road, Jinshui District, Zhengzhou 450003, China

* Corresponding author

E-mail: zhangweige2000@sina.com (W. Zhang), yingliang_1016@163.com (Y. Wu), guanqi@syphu.edu.cn (Q. Guan).

Abstract

A series of novel 3,5-diaryl-1*H*-pyrazolo[3,4-*b*]pyridines as tubulin polymerization inhibitors targeting the colchicine site were designed *via* ring tethering strategy, which was supported by conformational analysis. The general, chemically unstable and rotational linker, carbonyl group, was locked by 1*H*-pyrazolo[3,4-*b*]pyridine to avoid carbonyl reduction and restrict the instability of molecular conformation caused by the rotation of the carbon-carbon single bond beside carbonyl group. All of target compounds were synthesized and evaluated for their antiproliferative activities against three human cancer lines (SGC-7901, A549 and HeLa) by MTT assay. Most of these compounds showed prominent *in vitro* potency and the most potent compound in this scaffold **13d** (SGC-7901: IC₅₀ = 13 nM) could significantly inhibit tubulin polymerization and strongly disrupt cytoskeleton. The results of molecular modeling study revealed that **13d** interacts with tubulin by binding to the colchicine site.

Keywords: Ring tethering; Conformational analysis; Pyrazolo[3,4-*b*]pyridine; Colchicine site

1. Introduction

Microtubules are vital components of filamentous cytoskeleton consisted of α,β -tubulin heterodimers in eukaryotic cells.^[1] It is known that microtubules play important roles in driving many cellular physiological processes such as cell signaling, intracellular transport, intracellular macromolecular assemblies and cell division.^[2] The critical characteristic of microtubule is that it is always in a dynamic equilibrium of polymerization and depolymerization, and this is the foundation of tubulin polymerization inhibitors' functionality.^[3] The widely known tubulin polymerization inhibitors such as colchicine, CA-4 and SMART (Fig. 1) could be used for damaging or killing various types of tumor cells through breaking the equilibrium by binding to colchicine site in tubulin.^[4]

As SMART analogues, compounds **4-6** (Fig. 1) were designed according to bioisosterism and evaluated antiproliferative activity previously, with the IC_{50} values of 52-500 nM, 25-39 nM, >3000 nM, respectively.^[5] The loss of compound **6**'s activity impels us to explore the fundamental causes. Compared the chemical structures of compound **6** with **4**, **5** and SMART, they have a similar molecular skeleton containing three conjugated six-membered aromatic rings (A-, B-, and C-ring, respectively) with a ketone linker between A- and B-ring.^[6] Generally, structural modifications on B-ring using bioisosterism can be tolerated in maintaining original bioactivity.^[7] It is known that this antitubulin effect stems from the interactions between ligands (tubulin polymerization inhibitors) and receptor (α,β -tubulin) with appropriate binding mode. Therefore the difference of binding mode between **6** with the other compounds with α,β -tubulin may be the key point to explain the loss of activity of **6**. Unfortunately, co-crystal of SMART or its analogues with α,β -tubulin heterodimer complex has not been obtained up to now. Note that this class of compounds has two vastly different and relatively stable conformations, "bent" and "straight" conformation respectively (Fig. 2). Previously we reported that the "bent" conformation of SMART analogues may be critical for maintaining antitubulin activity based on the results of density functional theory (DFT).^[8] Inspired by this, we speculated that the difference of the preferred conformations of compounds **4-6** may be the reason that compound **6**'s low activity. To verify our speculation, DFT calculation was performed to compare the energy of two different conformations of the above compounds. As the results shown in Table 1, Compounds **3**, **4** and **5** may adopt stable "bent" conformation to interact with α,β -tubulin, which appears to be necessary

for potent biological activity. On the other hand, compound **6** has an entirely different and stable “straight” conformation and could not effectively interact with tubulin. Given the above analysis, “bent” conformation of molecule may be the key factor for the design of antitubulin inhibitors.

The pharmacokinetic behaviour of carbonyl group on SMART analogues is unstable because it can be easily reduced to hydroxyl *in vivo*, resulting in loss of bioactivities.^[9] Ring tethering strategy is an efficient means in drug design, which can be used for enhancing molecular stability through protecting sensitive group and restricting bioactive conformation. For example, CA-4 was often modified by the introduction of a five-membered aromatic heterocycle to lock the unstable *cis* carbon-carbon double bond.^[10-14]

1*H*-pyrazolo[3,4-*b*]pyridine is a special and significant fused aromatic heterocyclic ring, which has been used as a key pharmacophore in drug design. For example, BAY 41-2272 is a stimulator of soluble guanylate cyclase (sGC), which contains the 1*H*-pyrazolo[3,4-*b*]pyridine fragment;^[15] 6-Aryl pyrazolo[3,4-*b*]pyridine was also reported as inhibitor of glycogen synthase kinase-3 (GSK-3) in 2003.^[16]

Based on the above findings, a stable fragment 1*H*-pyrazolo[3,4-*b*]pyridine was chosen to replace the carbonyl linkage and B-ring through rational ring tethering strategy to restrict bioactive conformation and stabilize carbonyl group. Herein, a series of 3,5-diaryl-1*H*-pyrazolo[3,4-*b*]pyridines (**12a-m**, **13a-h**, and **13l-m**) were designed and synthesized as antitubulin agents (Fig. 3). The preliminary tests of bioactivity *in vitro*, including antiproliferative activity, tubulin polymerization, immunofluorescence staining, cell cycle analysis, and cytotoxicity test were performed to explore the preliminarily structure-activity relationship and illuminate the pharmacologic mechanism. Additionally, molecular modeling was carried out to investigate the possible binding mode of target compounds.

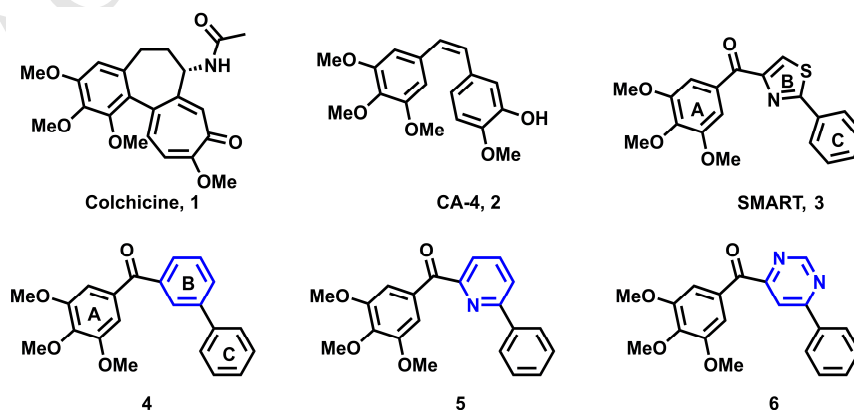
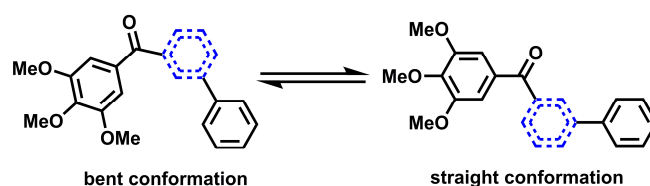
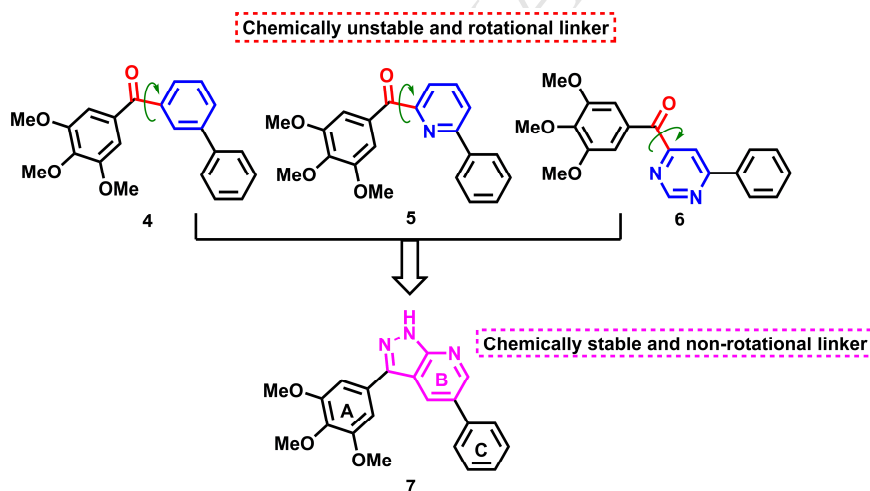


Fig. 1. Structures of colchicine, CA-4, SMART and analogues 4-6.**Fig. 2.** Two conformations of compounds 3-6 (the blue represent six-membered aromatic ring).**Table 1.** The relationships between conformation and bioactivity.

Compound	E_{bent} (a.u.) ^a	E_{straight} (a.u.)	$E_{\text{bent}}-E_{\text{straight}}$ (kJ/mol) ^b	IC ₅₀ (nM) ^c
SMART, 3	-1488.05297426	-1488.04806398	-12.89	21-71 (6 cell lines)
4	-1151.24384014	-1151.24359019	-0.66	52-500 (6 cell lines)
5	-1167.28482948	-1167.27773895	-18.62	25-39 (6 cell lines)
6	-1183.31988660	-1183.32631705	+16.88	>3000 (6 cell lines)

^a 1 a.u. = 2625.50 kJ/mol; ^b Negative value represents “bent” conformation is preferred conformation; ^c cited from literature [4].

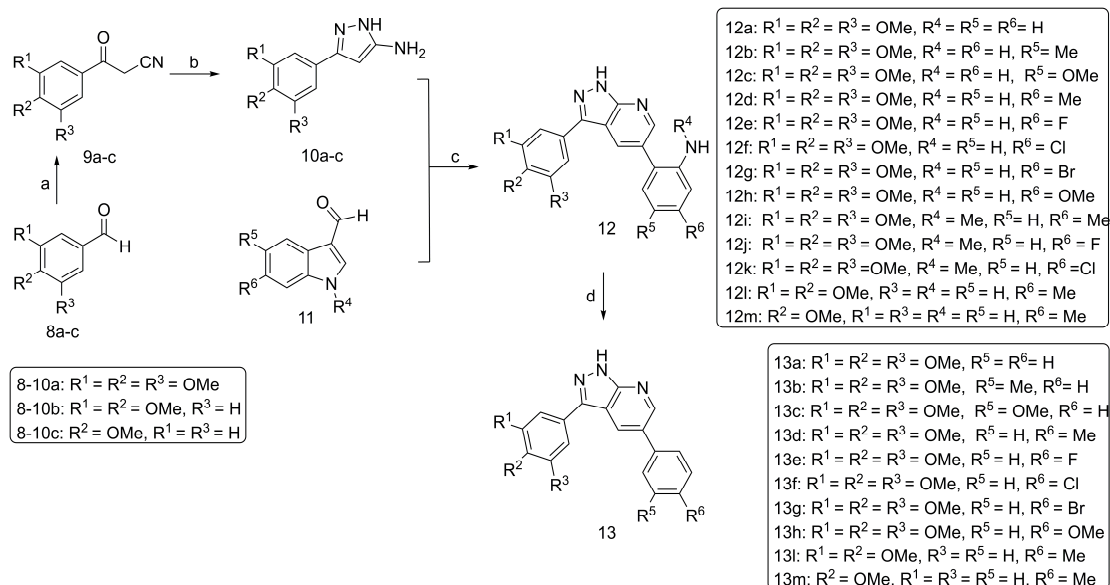
**Fig. 3.** Structure-based rational design *via* ring tethering strategy.

2. Results and discussion

2.1. Chemistry

The synthetic route for the target compounds (**12a-m**, **13a-h**, and **13l-m**) is outlined in Scheme 1. The key intermediate 3-(substituted phenyl)-1*H*-pyrazol-5-amine (compound **10**) was prepared in two steps. Briefly, the oxidative condensation of substituted benzaldehyde was carried out with acetonitrile to produce 3-oxo-3-(substituted phenyl)propanenitrile (compound **9**),^[17] followed by cyclization of compound **9** with 80% hydrazine hydrate in absolute ethanol.^[18] Subsequently, the

target compounds **12a-m** were obtained by treating compound **10** with corresponding indole-3-carboxaldehyde derivatives using direct one-step synthetic method.^[19] Finally, the amino-compounds **12a-h** were converted to the target compounds **13a-h** and **13l-m** via reductive deamination.^[20]



Scheme 1. Synthesis of the target compounds. Reagents and condition: (a) CuCl₂, KOH, CH₃CN, DMA, O₂ (balloon), rt, 24 h; (b) N₂H₄·H₂O (80%), TsOH, EtOH, reflux, 2 h; (c) AlCl₃, MeOH, 80°C, 4-8 h; (d) Isoamyl nitrite, THF, rt, 2-6 h.

2.2. Biological evaluation

2.2.1. *In vitro* antiproliferative activities and cytotoxicity assay

All the newly synthesized 3,5-diaryl-1*H*-pyrazolo[3,4-*b*]pyridines were screened against SGC-7901 (human gastric carcinoma cell line), A549 (human lung carcinoma cell line) and HeLa (Human cervical carcinoma cell line) by standard MTT assay to evaluate their antiproliferative activities in terms of half maximal inhibitory concentration (IC₅₀) values. By comparison, SMART was selected as the positive reference (Table 2). Obviously, the strategy of introducing fused-heterocyclic moiety is effective and almost all of the tested compounds exhibited moderate to potent antiproliferative activity except for compounds **12l-m** and **13l-m** (IC₅₀ > 30 μM), which have no 3,4,5-trimethoxyphenyl group. It can be seen that 3,4,5-trimethoxyphenyl group is a necessary pharmacophore for retaining bioactivities, which is consistent with previous reports about CA-4, SMART and its analogues.^[3] Compounds **12a-h** containing amino group at the C2-position of C-ring showed the IC₅₀ values of 0.081 to 10.25 μM. The antiproliferative activity

was reduced when the amino group of compounds **12d-f** was methylated. A clear growth of IC_{50} value was observed when the amino group of compounds **12a**, **12b** and **12d** was removed, and compound **13d** exhibited most potent antiproliferative activity against SGC-7901 cell with IC_{50} value of 13 nM, which was superior to SMART. The above analysis suggested that bulky substituents on C2-position of C-ring may be adverse. Compounds **12e-f** and **13e-f** possessing fluorine or chlorine atom at C4-position of C-ring were observed to be more active against HeLa and SGC-7901 cell lines in comparison with compounds **12g** and **13g**, which containing bromine atom at C4-position of C-ring. One possible reason for this phenomenon was that the bromine atom has lower electronegativity and bigger atom size. Meanwhile, one of most distinct characteristics of these compounds was that they exhibited selective antiproliferative activities on different tumor cell lines. For example, compounds **12b**, **12d-f**, **13b** and **13h** showed strong and selective inhibition to the proliferation of HeLa and SGC-7901 cell lines (IC_{50} value 0.013-0.62 μ M) while A549 cell line was not sensitive to these compounds ($IC_{50} > 1.31 \mu$ M).

Table 2. Antiproliferative activities of target compounds.

Compounds	$(IC_{50} \pm SD, \mu M)^a$		
	SGC-7901	A549	HeLa
12a	4.37 \pm 0.18	1.42 \pm 0.09	2.55 \pm 0.11
12b	0.62 \pm 0.05	4.43 \pm 0.24	0.38 \pm 0.02
12c	9.51 \pm 0.87	10.25 \pm 1.02	4.93 \pm 0.77
12d	0.23 \pm 0.021	7.83 \pm 0.45	0.16 \pm 0.011
12e	0.40 \pm 0.017	1.31 \pm 0.10	0.081 \pm 0.008
12f	0.58 \pm 0.024	3.24 \pm 0.18	0.36 \pm 0.017
12g	5.52 \pm 0.16	8.47 \pm 0.23	2.61 \pm 0.12
12h	3.73 \pm 0.14	5.36 \pm 0.24	1.44 \pm 0.49
12i	6.31 \pm 0.39	9.25 \pm 0.44	3.84 \pm 0.15
12j	3.76 \pm 0.21	4.27 \pm 0.20	1.67 \pm 0.37
12k	8.48 \pm 0.76	14.02 \pm 1.03	6.49 \pm 0.70
12l	>30	>30	>30
12m	>30	>30	>30

13a	0.037 ± 0.004	0.65 ± 0.043	0.057 ± 0.007
13b	0.051 ± 0.006	>30	0.086 ± 0.012
13c	1.91 ± 0.21	7.66 ± 0.48	0.46 ± 0.025
13d	0.013 ± 0.005	0.082 ± 0.016	0.045 ± 0.008
13e	2.31 ± 0.17	>30	0.89 ± 0.12
13f	4.82 ± 0.96	14.61 ± 1.24	0.87 ± 0.15
13g	20.15 ± 1.78	17.43 ± 1.10	10.86 ± 1.97
13h	0.13 ± 0.010	>30	0.28 ± 0.016
13i	>30	>30	>30
13m	>30	>30	>30
SMART (3) ^b	0.018 ± 0.006	0.029 ± 0.009	0.024 ± 0.011

^aData from three independent experiments; ^bUsed as positive control.

Next, cytotoxicity test was carried out by using normal fibroblasts L929 cell line to assess the cytotoxicity of the most potent compound **13d** against non-tumor cells, and SMART was utilized as positive control. As shown in Table 3, the data demonstrated that the cytotoxicity of compound **13d** (IC₅₀ value 37.5 μM) was obviously weaker than SMART (IC₅₀ value 25.8 μM).

Table 3. Cytotoxicity test of compound **13d** and SMART against L929 cells.

Compound	(IC ₅₀ ± SD, μM)
13d	37.5 ± 2.4
SMART	25.8 ± 2.0

2.2.2. Tubulin polymerization *in vitro*

In order to shed light on the biological mechanism of this series of compounds, the most potent compound **13d** was selected to examine the antitubulin activity, meanwhile SMART was used as positive control and taxol, the first compound known to interact with and stabilize tubulin, was utilized as negative control. As shown in Fig. 4, **13d** significantly exhibited antitubulin activity which was very close to SMART. Additionally, compound **13d** inhibited tubulin polymerization in a dose-dependent manner. These data indicated that this series of compounds most likely targeted at tubulin.

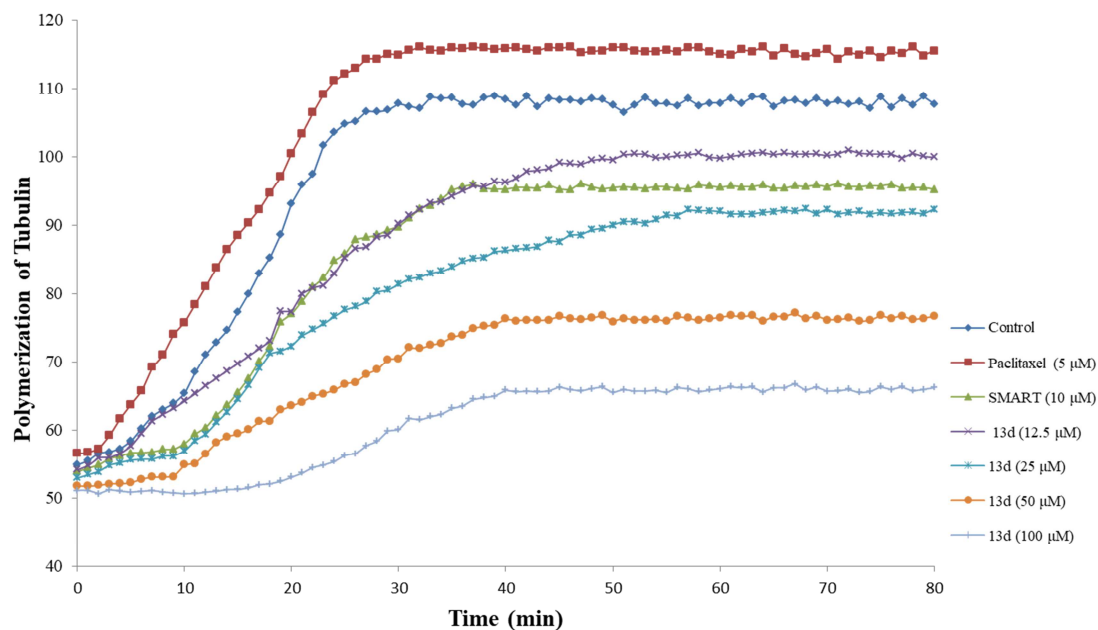


Fig. 4. Effects of compound **13d** (12.5-100 μM), paclitaxel (5 μM), and SMART (10 μM) on tubulin polymerization *in vitro*. The assay was performed using a fluorescence-based tubulin polymerization assay kit (Cytoskeleton-Cat. #BK011P). Absorbance was monitored at 37°C every minute for 80 min.

2.2.3. Immunofluorescence staining of tubulin

To further investigate the impacts of **13d** on intracellular microtubules, SGC-7901 cell was utilized for immunofluorescence assay to directly observe the changes in morphology of microtubules and SMART was utilized as reference. As shown in Fig. 5, the microtubule network (green) in normal SGC-7901 cells was well-assembled and evenly distributed in cytoplasm. Treatment of SGC-7901 cells with 36 nM (2-fold IC_{50}) of SMART and 26 nM (2-fold IC_{50}) of compound **13d** for 24 h, respectively, led to profound changes of the microscopic shape and structure. The changes were outstandingly shown in two interrelated aspects: one is that the cytoskeleton was destroyed and cell morphology became round; another one is the presence of multinucleated cells. This phenomenon means that compound **13d** may be a colchicine site binder, similar to SMART.

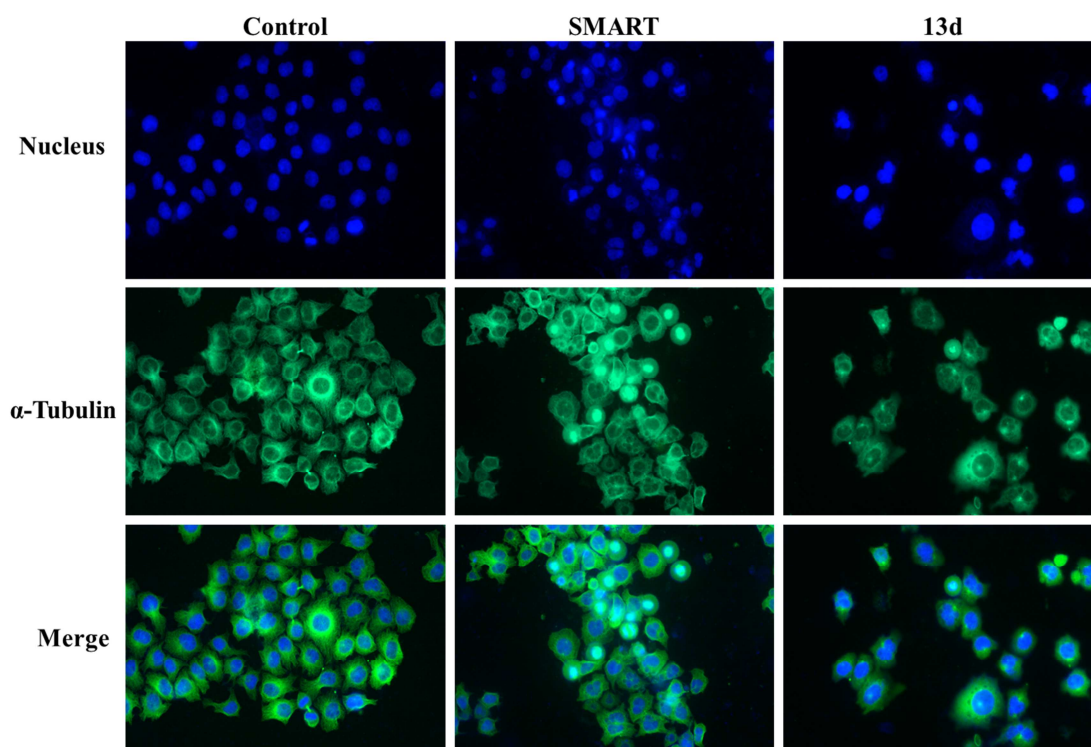


Fig. 5. Effects of SMART (36 nM) and **13d** (26 nM) on the morphology of SGC-7901 cells by immunofluorescence assay. Microtubule and unassembled tubulin were stained green; nuclei were stained blue.

2.2.4. Cell cycle arrest

It was known that tubulin polymerization inhibitors could trigger the alteration of cell cycle parameters resulting in a preferential G2/M blockade. Therefore, cell cycle analysis assay was performed to investigate the effects of the most potent compound **13d** on the cell cycle (Fig. 6). SGC-7901 cells were incubated with SMART (36 nM, Fig. 6A) or **13d** (26 nM, Fig. 6B), and the proportion of tested cells at different cell cycle phases was analyzed by flow cytometry after 0, 12, 24, 36, 48, and 72 h of treatment, respectively. As the results depicted in Fig. 6A, SMART induced a sharply decrease of G1 cell population, and an increase of G2/M cell population. Meanwhile, massive multinucleated cells were observed, which was consistent with the immunofluorescence assay. As shown in Fig. 6B, the G2/M cell population increased significantly from 24.47% to 59.62% after treatment with 26 nM of **13d** for 12 h. Thus, the cell cycle distribution indicated that compound **13d** could arrest SGC-7901 cell in G2/M phase.

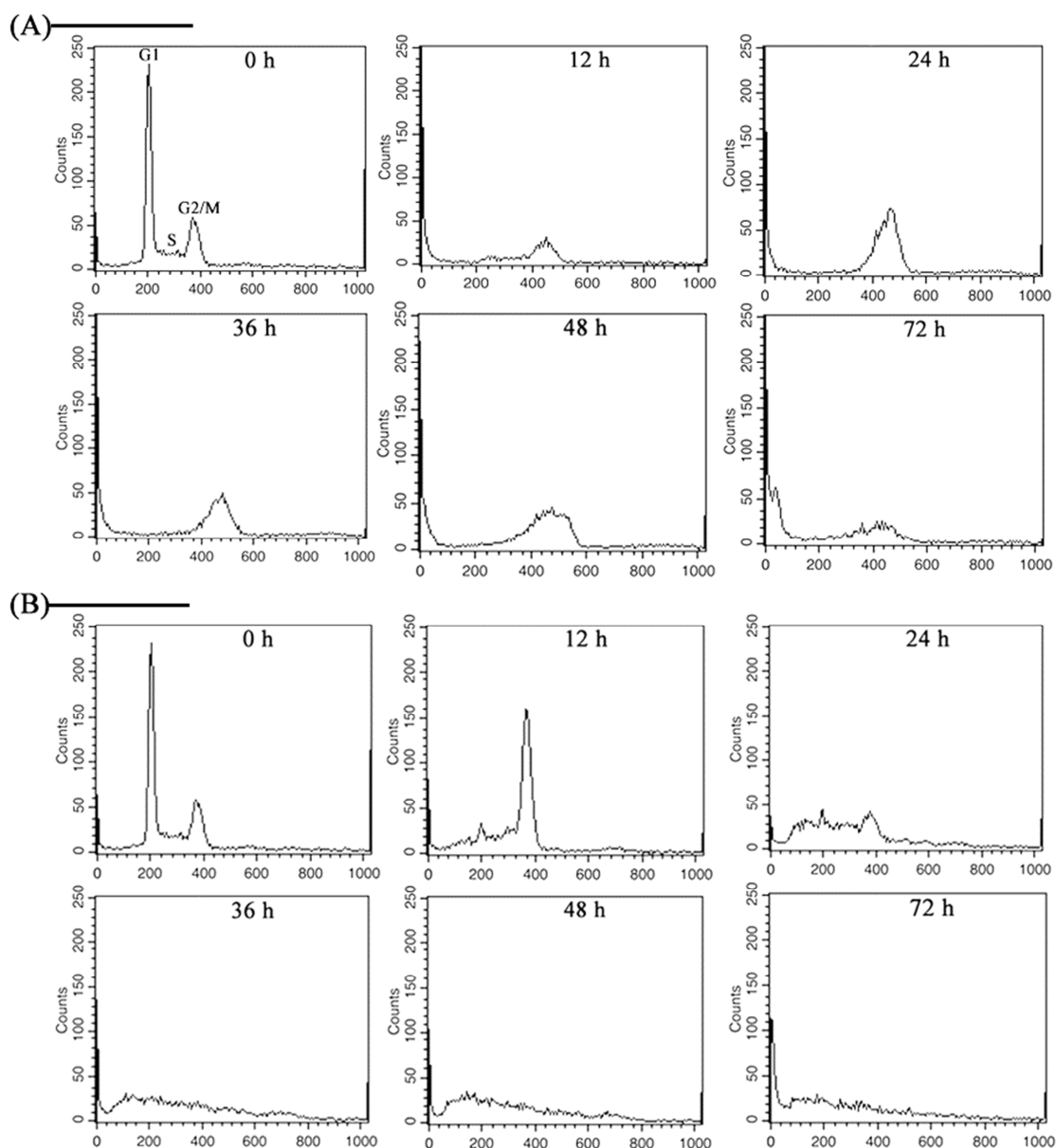


Fig. 6. The effects of SMART (6A) and **13d** (6B) on the cell cycle distributions.

2.3. Molecular modeling

For the aim to research the potential binding mode of the target compounds, the most potent compound **13d** was docked into the tubulin-CA-4 complex (PDB code: 5LYJ) by following the procedure of our previous report.^[8] The docking-derived superimposition of **13d** (green), **4** (purple), and **5** (yellow) was illustrated in the Fig. 7A. **13d** showed a binding pose similar to compounds **4** and **5**, and the molecular skeletons of these three could be well superimposed. As the 2D diagram of **13d**-tubulin interactions shown in Fig. 7B, the oxygen atom of methoxyl group at C4-position of A-ring which located in β -tubulin deeply could establish a hydrogen bond with β -Cys241 (2.17 Å). Meanwhile, the methyl group at C4-position of C-ring which extended toward

α -tubulin could form alkyl hydrophobic interaction with α -Val181 (3.57 Å). The docking results suggested that **13d** may exhibit its biological activities by binding to colchicine site.

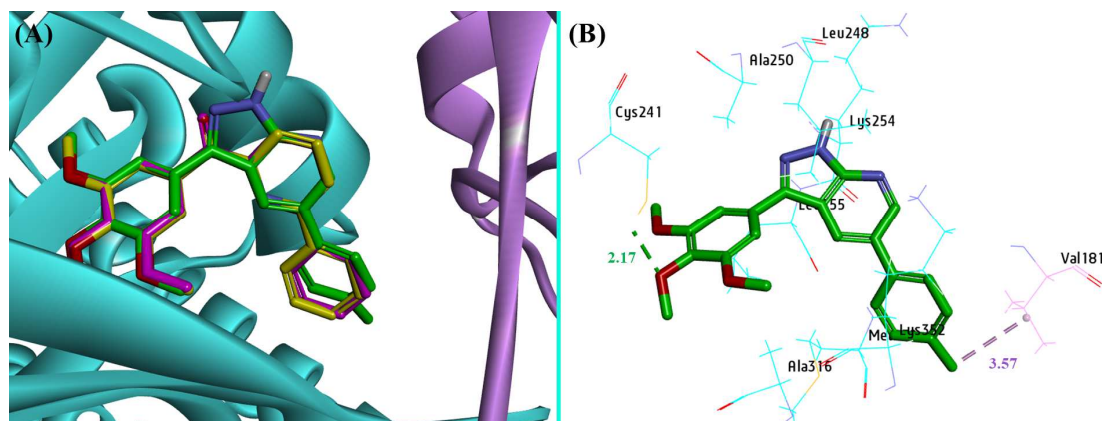


Fig. 7. (A) Possible binding modes of compound **4**, **5** and **13d** in colchicine site (purple-**4**; yellow-**5**; green-**13d**); (B) Compound **13d**-tubulin interactions (green dotted line represents hydrogen bond, purple dotted line represents alkyl hydrophobic interaction). All of the nonpolar hydrogen atoms were removed for the purpose of clarity.

3. Conclusion

A new series of 3,5-diaryl-1*H*-pyrazolo[3,4-*b*]pyridines was designed rationally through the strategy of ring tethering which was supported by the conformational analysis. All of the designed compounds **12a-12m**, **13a-13h**, and **13i-13m** were synthesized and characterized. MTT assay was used to evaluate the antiproliferative activity preliminarily against three human tumor cells (SGC-7901, A549, and HeLa) and most of the target compounds showed potent inhibitory activity at sub-micromolar to nanomolar level. The most potent compound **13d** was selected to illuminate the biological mechanism through tubulin polymerization assay, immunofluorescence staining, and cell cycle analysis. Results indicated that **13d** could inhibit tubulin assembly effectively *in vitro*, destroy the skeleton of intracellular microtubule significantly, and induce cell cycle arrest in G2/M phase. Furthermore, molecular modeling studies showed that **13d** could bind to colchicine site strongly. More importantly, this successful instance of molecular design based on conformation revealed that “bent” conformation is a critical factor in the rational design of SMART analogues. In addition, we believe that some chain or ring-like polar fragments which are beneficial to maintain the “bent” conformation of SMART analogues can probably be introduced on B-ring to adjust the physicochemical properties so as to meet the requirements of druggability. It will be our main objective which should be researched continuously and the correlational study will be duly published.

4. Experimental section

4.1. Chemistry

All of reagents and solvents were purchased from chemical company. TLC analysis was used for determining the extent of reactions under UV light (wavelength: 365 nm and 254 nm). ^1H (600 MHz) and ^{13}C NMR (150 MHz) spectra were tested on a Bruker AVANCE 600 by using DMSO- d_6 or CDCl_3 as solvent (0.03% TMS as internal reference) at room temperature. Melting point was measured (uncorrected) on hot-stage microscope (Beijing Taike, X-4). Mass spectra were performed on an Agilent 1100-sl mass spectrometer with electrospray ionization (ESI) source from Agilent Co.Ltd. High resolution mass determinations (HRMS) for target compounds were obtained on an Agilent 6530 accurate-mass Q-TOF LC-MS system.

4.1.1. Synthesis of intermediates **9a-c**

The mixture of **8** (10 mmol), CH_3CN (100 mmol), CuCl_2 (0.3 mmol) and KOH (30 mmol) in *N,N*-dimethylacetamide (DMA) was stirred vigorously under O_2 atmosphere at 25°C for 24 h. When the reaction was completed, the volatile solvent was removed under reduced pressure and the unsolvable impurities were excluded by filter. 200 mL water was added into the filtrate, then the pH was adjusted to 7 by slowly adding 20% hydrochloric acid and massive amounts of solid precipitated out. Finally, the solid was collected by filtration and washed three times with water to furnish intermediates **9a-c** as white solid with yield ranged from 72% to 76%.

4.1.1.1. 3-oxo-3-(3,4,5-trimethoxyphenyl)propanenitrile (**9a**)

White solid, yield 75%, ^1H NMR (600 MHz, CDCl_3): δ 3.93 (6H, s), 3.95 (3H, s), 4.08 (2H, s), 7.15 (2H, s). MS (ESI): $[\text{M}+\text{H}]^+ = 236.1$.

4.1.1.2. 3-oxo-3-(3,4-dimethoxyphenyl)propanenitrile (**9b**)

White solid, yield 76%, ^1H NMR (600 MHz, CDCl_3): δ 3.95 (s, 3H), 3.98 (s, 3H), 4.04 (s, 2H), 6.92 (d, $J = 8.0$ Hz, 1H), 7.49 (d, $J = 8.0$ Hz, 1H), 7.51 (s, 1H). MS (ESI): $[\text{M}+\text{H}]^+ = 206.0$.

4.1.1.3. 3-oxo-3-(4-methoxyphenyl)propanenitrile (**9c**)

White solid, yield 72%, ^1H NMR (600 MHz, CDCl_3): δ 3.90 (s, 3H), 4.03 (s, 2H), 6.98 (d, $J = 8.9$ Hz, 2H), 7.90 (d, $J = 8.9$ Hz, 2H). MS (ESI): $[\text{M}+\text{H}]^+ = 176.1$

4.1.2. Synthesis of key intermediates **10a-c**

To a solution of **9** (5 mmol) and *p*-toluenesulfonic acid (TsOH, 0.1 mmol) in ethanol was added 80% hydrazine hydrate dropwise at 78°C . On completion of the reaction (TLC check), the

solvent was removed under reduced pressure and the crude product was purified by silica gel column chromatography to afford intermediates **10a-c** as white solid in excellent yields.

4.1.2.1. 3-(3,4,5-Trimethoxyphenyl)-1*H*-pyrazol-5-amine (**10a**)

White solid, yield 93%, ¹H NMR (600 MHz, DMSO-*d*₆): δ 3.66 (s, 3H), 3.81 (s, 6H), 4.75 (brs, 2H), 5.78 (s, 1H), 6.95 (s, 2H), 11.70 (brs, 1H). MS (ESI): [M+H]⁺ = 250.1, [M+Na]⁺ = 272.1.

4.1.2.2. 3-(3,4-Dimethoxyphenyl)-1*H*-pyrazol-5-amine (**10b**)

White solid, yield 93%, ¹H NMR (600 MHz, DMSO-*d*₆): δ 3.76 (s, 3H), 3.79 (s, 3H), 4.71 (brs, 2H), 5.71 (s, 1H), 6.94 (d, *J* = 8.3 Hz, 1H), 7.16 (dd, *J* = 8.3, 1.9 Hz, 1H), 7.24 (d, *J* = 1.9 Hz, 1H), 11.63 (brs, 1H). MS (ESI): [M+H]⁺ = 220.1.

4.1.2.3. 3-(3-Methoxyphenyl)-1*H*-pyrazol-5-amine (**10c**)

White solid, yield 95%, ¹H NMR (600 MHz, DMSO-*d*₆): δ 3.76 (s, 3H), 4.70 (brs, 2H), 5.68 (s, 1H), 6.94 (d, *J* = 8.6 Hz, 2H), 7.57 (d, *J* = 8.6 Hz, 2H), 11.68 (brs, 1H). MS (ESI): [M+H]⁺ = 190.1.

4.1.3. Synthesis of target compounds **12a-m**

To a solution of **10** (0.5 mmol) and 1*H*-indole-3-carbaldehyde derivatives **11** (0.5 mmol) in 2 mL anhydrous methanol, AlCl₃ (0.05 mmol) was added then the mixture was stirred for 4-8 h in 15 mL heavy-wall pressure vessel at 70°C. When the completion of reaction (TLC check), the mixture was naturally cooled to room temperature, and the resulting solid was filtered. The crude product was purified by silica gel column chromatography or recrystallization in ethyl acetate to afford target compounds **12a-m** as white solid with yield ranged from 56% to 75%.

4.1.3.1. 2-(3-(3,4,5-Trimethoxyphenyl)-1*H*-pyrazolo[3,4-*b*]pyridin-5-yl)aniline (**12a**)

White solid, yield 78%, mp 214-216°C, ¹H NMR (600 MHz, DMSO-*d*₆): δ 3.72 (s, 3H), 3.88 (s, 6H), 5.04 (s, 2H), 6.66-6.69 (m, 1H), 6.79 (d, *J* = 8.1 Hz, 1H), 7.07-7.10 (m, 1H), 7.12 (d, *J* = 7.4 Hz, 1H), 7.25 (s, 2H), 8.48 (s, 1H), 8.56 (s, 1H), 13.81 (s, 1H); ¹³C NMR (150 MHz, DMSO-*d*₆): δ 56.5 (2C), 60.6, 104.6 (2C), 112.5, 115.9, 117.3, 123.2, 129.0, 129.3, 129.4, 130.0, 131.3, 138.1, 143.4, 146.5, 150.3, 152.4, 153.8 (2C). HRMS (ESI): calcd. for C₂₁H₂₀N₄NaO₃ [M+Na]⁺ 399.1428, found 399.1432.

4.1.3.2. 4-Methyl-2-(3-(3,4,5-trimethoxyphenyl)-1*H*-pyrazolo[3,4-*b*]pyridin-5-yl)aniline (**12b**)

White solid, yield 64%, mp 192-193°C, ¹H NMR (600 MHz, DMSO-*d*₆): δ 2.21 (s, 3H), 3.73 (s, 3H), 3.88 (s, 6H), 4.95 (s, 2H), 6.73 (d, *J* = 8.3 Hz, 1H), 6.92 (d, *J* = 8.3 Hz, 1H), 6.96 (s, 1H),

7.24 (s, 2H), 8.48 (s, 1H), 8.56 (s, 1H), 13.81 (s, 1H); ^{13}C NMR (150 MHz, DMSO- d_6): δ 20.5, 56.5 (2C), 60.6, 104.7 (2C), 112.4, 116.3, 123.4, 126.0, 129.3, 129.4, 129.5, 129.9, 131.7, 138.1, 143.4, 143.6, 150.3, 152.4, 153.8 (2C). HRMS (ESI): calcd. for $\text{C}_{22}\text{H}_{22}\text{N}_4\text{NaO}_3$ $[\text{M}+\text{Na}]^+$ 413.1584, found 413.1589.

4.1.3.3. 4-Methoxy-2-(3-(3,4,5-trimethoxyphenyl)-1H-pyrazolo[3,4-b]pyridin-5-yl)aniline (**12c**)

White solid, yield 75%, mp 208-210°C, ^1H NMR (600 MHz, DMSO- d_6): δ 3.69 (s, 3H), 3.73 (s, 3H), 3.89 (s, 6H), 4.63 (s, 2H), 6.74-6.79 (m, 3H), 7.25 (s, 2H), 8.53 (d, $J = 1.4$ Hz, 1H), 8.62 (d, $J = 1.4$ Hz, 1H), 13.82 (s, 1H); ^{13}C NMR (150 MHz, DMSO- d_6): δ 55.8, 56.5 (2C), 60.6, 104.6 (2C), 112.4, 115.2, 116.3, 117.3, 124.2, 129.3, 129.4, 130.1, 138.1, 140.1, 143.5, 150.3, 151.9, 152.4, 153.8 (2C). HRMS (ESI): calcd. for $\text{C}_{22}\text{H}_{23}\text{N}_4\text{O}_4$ $[\text{M}+\text{H}]^+$ 407.1714, found 407.1717; $\text{C}_{22}\text{H}_{22}\text{N}_4\text{NaO}_4$ $[\text{M}+\text{Na}]^+$ 429.1533, found 429.1537.

4.1.3.4. 5-Methyl-2-(3-(3,4,5-trimethoxyphenyl)-1H-pyrazolo[3,4-b]pyridin-5-yl)aniline (**12d**)

White solid, yield 63%, mp 180-182°C, ^1H NMR (600 MHz, DMSO- d_6): δ 2.22 (s, 3H), 3.73 (s, 3H), 3.88 (s, 6H), 4.96 (s, 2H), 6.50 (d, $J = 7.5$ Hz, 1H), 6.62 (s, 1H), 7.01 (d, $J = 7.5$ Hz, 1H), 7.24 (s, 2H), 8.44 (d, $J = 1.6$ Hz, 1H), 8.54 (d, $J = 1.6$ Hz, 1H), 13.79 (s, 1H); ^{13}C NMR (150 MHz, DMSO- d_6): δ 21.4, 56.4 (2C), 60.6, 104.6 (2C), 112.5, 116.4, 118.3, 120.6, 129.3, 129.4, 129.9, 131.2, 138.0, 138.1, 143.3, 146.2, 150.3, 152.4, 153.8 (2C). HRMS (ESI): calcd. for $\text{C}_{22}\text{H}_{22}\text{N}_4\text{NaO}_3$ $[\text{M}+\text{Na}]^+$ 413.1584, found 413.1588.

4.1.3.5. 5-Fluoro-2-(3-(3,4,5-trimethoxyphenyl)-1H-pyrazolo[3,4-b]pyridin-5-yl)aniline (**12e**)

White solid, yield 56%, mp 223-224°C, ^1H NMR (600 MHz, DMSO- d_6): δ 3.73 (s, 3H), 3.88 (s, 6H), 5.38 (s, 2H), 6.43-6.46 (m, 1H), 6.57 (d, $J = 11.1$ Hz, 1H), 7.12-7.14 (m, 1H), 7.25 (s, 2H), 8.45 (s, 1H), 8.52 (s, 1H), 13.82 (s, 1H); ^{13}C NMR (150 MHz, DMSO- d_6): δ 56.5 (2C), 60.6, 101.5 (d, $J = 23.9$ Hz), 103.4 (d, $J = 21.6$ Hz), 104.6 (2C), 112.5, 119.6, 128.4, 129.3, 130.3, 132.8 (d, $J = 10.3$ Hz), 138.1, 143.4, 148.5 (d, $J = 11.7$ Hz), 150.3, 152.5, 153.8 (2C), 164.1 (d, $J = 238.8$ Hz). HRMS (ESI): calcd. for $\text{C}_{21}\text{H}_{20}\text{FN}_4\text{O}_3$ $[\text{M}+\text{H}]^+$ 395.1514, found 395.1525; $\text{C}_{21}\text{H}_{19}\text{FN}_4\text{NaO}_3$ $[\text{M}+\text{Na}]^+$ 417.1333, found 417.1351.

4.1.3.6. 5-Chloro-2-(3-(3,4,5-trimethoxyphenyl)-1H-pyrazolo[3,4-b]pyridin-5-yl)aniline (**12f**)

White solid, yield 69%, mp 227-229°C, ^1H NMR (600 MHz, DMSO- d_6): δ 3.73 (s, 3H), 3.88 (s, 6H), 5.39 (s, 2H), 6.66 (d, $J = 7.7$ Hz, 1H), 6.84 (s, 1H), 7.12 (d, $J = 7.7$ Hz, 1H), 7.24 (s, 2H), 8.47 (s, 1H), 8.53 (s, 1H), 13.84 (s, 1H); ^{13}C NMR (150 MHz, DMSO- d_6): δ 56.5 (2C), 60.6,

104.6 (2C), 112.5, 114.7, 116.5, 122.0, 128.2, 129.2, 130.2, 132.8, 133.4, 138.1, 143.5, 148.2, 150.1, 152.5, 153.8 (2C). HRMS (ESI): calcd. for $C_{21}H_{20}ClN_4O_3$ $[M+H]^+$ 411.1218, found 411.1217; $C_{21}H_{19}ClN_4NaO_3$ $[M+Na]^+$ 433.1038, found 433.1056.

4.1.3.7. 5-Bromo-2-(3-(3,4,5-trimethoxyphenyl)-1*H*-pyrazolo[3,4-*b*]pyridin-5-yl)aniline (**12g**)

White solid, yield 61%, mp 132-134°C, 1H NMR (600 MHz, DMSO- d_6): δ 3.72 (s, 3H), 3.88 (s, 6H), 5.37 (s, 2H), 6.79 (dd, $J = 8.0$ Hz, $J = 2.0$ Hz, 1H), 6.98 (d, $J = 2.0$ Hz, 1H), 7.05 (d, $J = 8.0$ Hz, 1H), 7.24 (s, 2H), 8.46 (d, $J = 1.9$ Hz, 1H), 8.52 (d, $J = 1.9$ Hz, 1H), 13.83 (s, 1H); ^{13}C NMR (150 MHz, DMSO- d_6): δ 56.5 (2C), 60.6, 104.6 (2C), 112.4, 117.6, 119.3, 122.0, 128.2, 129.2, 129.8, 130.2, 133.1, 138.1, 143.5, 148.4, 150.1, 152.5, 153.8 (2C). HRMS (ESI): calcd. for $C_{21}H_{20}BrN_4O_3$ $[M+H]^+$ 455.0713, found 455.0723.

4.1.3.8. 5-Methoxy-2-(3-(3,4,5-trimethoxyphenyl)-1*H*-pyrazolo[3,4-*b*]pyridin-5-yl)aniline (**12h**)

White solid, yield 65%, mp 202-204°C, 1H NMR (600 MHz, DMSO- d_6): δ 3.72 (s, 3H), 3.73 (s, 3H), 3.88 (s, 6H), 5.08 (s, 2H), 6.28 (dd, $J = 8.6$ Hz, $J = 2.5$ Hz, 1H), 6.39 (d, $J = 2.5$ Hz, 1H), 7.04 (d, $J = 8.6$ Hz, 1H), 7.24 (s, 2H), 8.42 (d, $J = 1.9$ Hz, 1H), 8.53 (d, $J = 1.9$ Hz, 1H), 13.77 (s, 1H); ^{13}C NMR (150 MHz, DMSO- d_6): δ 55.2, 56.4 (2C), 60.6, 100.9, 103.4, 104.6 (2C), 112.5, 116.4, 129.2, 129.4, 129.8, 132.1, 138.1, 143.3, 147.6, 150.4, 152.3, 153.8 (2C), 160.4. HRMS (ESI): calcd. for $C_{22}H_{22}N_4NaO_4$ $[M+Na]^+$ 429.1533, found 429.1557.

4.1.3.9. *N*,5-dimethyl-2-(3-(3,4,5-trimethoxyphenyl)-1*H*-pyrazolo[3,4-*b*]pyridin-5-yl)aniline (**12i**)

White solid, yield 75%, mp 232-234°C, 1H NMR (600 MHz, DMSO- d_6): δ 2.30 (s, 3H), 2.65 (d, $J = 5.0$ Hz, 3H), 3.72 (s, 3H), 3.88 (s, 6H), 5.18 (q, $J = 5.0$ Hz, 2H), 6.47 (s, 1H), 6.52 (d, $J = 7.4$ Hz, 1H), 7.00 (d, $J = 7.4$ Hz, 1H), 7.23 (s, 2H), 8.40 (d, $J = 1.9$ Hz, 1H), 8.48 (d, $J = 1.9$ Hz, 1H), 13.80 (s, 1H); ^{13}C NMR (150 MHz, DMSO- d_6): δ 21.9, 30.6, 56.4 (2C), 60.6, 104.6 (2C), 111.0, 112.5, 117.3, 121.4, 129.0, 129.3, 130.1, 130.4, 131.0, 138.1, 143.4, 147.4, 150.6, 152.5, 153.8 (2C). HRMS (ESI): calcd. for $C_{23}H_{25}N_4O_3$ $[M+H]^+$ 405.1921, found 405.1929; $C_{23}H_{24}N_4NaO_3$ $[M+Na]^+$ 427.1741, found 427.1748.

4.1.3.10. 5-Fluoro-*N*-methyl-2-(3-(3,4,5-trimethoxyphenyl)-1*H*-pyrazolo[3,4-*b*]pyridin-5-yl)aniline (**12j**)

White solid, yield 66%, mp 260-262°C, 1H NMR (600 MHz, DMSO- d_6): δ 2.65 (d, $J = 4.8$ Hz, 3H), 3.72 (s, 3H), 3.88 (s, 6H), 5.55 (q, $J = 4.8$ Hz, 1H), 6.40-6.42 (m, 1H), 6.45-6.48 (m, 1H), 7.10-7.13 (m, 1H), 7.24 (s, 2H), 8.41 (d, $J = 1.7$ Hz, 1H), 8.47 (d, $J = 1.7$ Hz, 1H), 13.83 (s, 1H);

^{13}C NMR (150 MHz, DMSO- d_6): δ 30.5, 56.4 (2C), 60.6, 97.0 (d, $J = 26.0$ Hz), 102.1 (d, $J = 21.6$ Hz), 104.7 (2C), 112.6, 120.3 (d, $J = 1.7$ Hz), 128.1, 129.2, 130.8, 132.4 (d, $J = 10.4$ Hz), 138.1, 143.5, 149.6 (d, $J = 11.4$ Hz), 150.6, 152.6, 153.8 (2C), 164.0 (d, $J = 241.3$ Hz). HRMS (ESI): calcd. for $\text{C}_{22}\text{H}_{21}\text{FN}_4\text{NaO}_3$ $[\text{M}+\text{Na}]^+$ 431.1490, found 431.1502.

4.1.3.11. 5-Chloro-*N*-methyl-2-(3-(3,4,5-trimethoxyphenyl)-1*H*-pyrazolo[3,4-*b*]pyridin-5-yl)aniline (**12k**)

Pale yellow solid, yield 72%, mp 269-271°C, ^1H NMR (600 MHz, DMSO- d_6): δ 2.65 (d, $J = 4.7$ Hz, 3H), 3.72 (s, 3H), 3.88 (s, 6H), 5.56 (q, $J = 4.7$ Hz, 1H), 6.60 (d, $J = 1.8$ Hz, 1H), 6.70 (dd, $J = 7.9$ Hz, $J = 1.8$ Hz, 1H), 7.11 (d, $J = 7.9$ Hz, 1H), 7.23 (s, 2H), 8.42 (d, $J = 1.7$ Hz, 1H), 8.48 (d, $J = 1.7$ Hz, 1H), 13.84 (s, 1H); ^{13}C NMR (150 MHz, DMSO- d_6): δ 30.4, 56.4 (2C), 60.6, 104.7 (2C), 109.6, 112.5, 115.7, 122.9, 127.8, 129.2, 130.8, 132.5, 134.3, 138.1, 143.6, 149.0, 150.4, 152.7, 153.8 (2C). HRMS (ESI): calcd. for $\text{C}_{22}\text{H}_{22}\text{ClN}_4\text{O}_3$ $[\text{M}+\text{H}]^+$ 425.1375, found 425.1384.

4.1.3.12. 2-(3-(3,4-dimethoxyphenyl)-1*H*-pyrazolo[3,4-*b*]pyridin-5-yl)-5-methylaniline (**12l**)

White solid, yield 68%, mp 239-241°C, ^1H NMR (600 MHz, DMSO- d_6): δ 2.22 (s, 3H), 3.82 (s, 3H), 3.86 (s, 3H), 4.91 (s, 2H), 6.50 (dd, $J = 7.5$ Hz, $J = 0.9$ Hz, 1H), 6.62 (s, 1H), 6.99 (d, $J = 7.5$ Hz, 1H), 7.09 (d, $J = 8.0$ Hz, 2H), 7.56-7.57 (m, 2H), 8.42 (d, $J = 1.9$ Hz, 1H), 8.52 (d, $J = 1.9$ Hz, 1H), 13.70 (s, 1H); ^{13}C NMR (150 MHz, DMSO- d_6): δ 21.4, 55.9, 56.0, 110.3, 112.4, 112.5, 116.3, 118.3, 119.8, 120.7, 126.5, 129.3, 130.0, 131.2, 138.1, 143.2, 146.2, 149.4, 149.5, 150.2, 152.4. HRMS (ESI): calcd. for $\text{C}_{21}\text{H}_{20}\text{N}_4\text{NaO}_2$ $[\text{M}+\text{Na}]^+$ 383.1478, found 383.1498.

4.1.3.13. 2-(3-(4-methoxyphenyl)-1*H*-pyrazolo[3,4-*b*]pyridin-5-yl)-5-methylaniline (**12m**)

White solid, yield 65%, mp 236-238°C, ^1H NMR (600 MHz, DMSO- d_6): δ 2.23 (s, 3H), 3.82 (s, 3H), 4.89 (s, 2H), 6.50 (dd, $J = 7.6$ Hz, $J = 0.7$ Hz, 1H), 6.62 (s, 1H), 6.99 (d, $J = 7.6$ Hz, 1H), 7.08 (d, $J = 8.7$ Hz, 2H), 7.97 (d, $J = 8.7$ Hz, 2H), 8.40 (d, $J = 1.8$ Hz, 1H), 8.52 (d, $J = 1.8$ Hz, 1H), 13.69 (s, 1H); ^{13}C NMR (150 MHz, DMSO- d_6): δ 21.4, 55.6, 112.4, 114.9 (2C), 116.2, 118.2, 120.8, 126.4, 128.4 (2C), 129.3, 130.0, 131.2, 138.1, 143.1, 146.2, 150.1, 152.4, 159.7. HRMS (ESI): calcd. for $\text{C}_{20}\text{H}_{18}\text{N}_4\text{NaO}$ $[\text{M}+\text{Na}]^+$ 353.1373, found 353.1397.

4.1.4. Synthesis of target compounds **13a-h**

The mixture of **12** (0.2 mmol) and isoamyl nitrite (0.3 mmol) in THF was stirred for 2-6 h at room temperature. The solvent was removed under reduced pressure and the residue was purified

by silica gel column chromatography to afford target compounds **13a-h** as white solid with yield ranged from 64% to 83%.

4.1.4.1. 5-Phenyl-3-(3,4,5-trimethoxyphenyl)-1*H*-pyrazolo[3,4-*b*]pyridine (**13a**)

White solid, yield 72%, mp 172-174°C, ¹H NMR (600 MHz, DMSO-*d*₆): δ 3.79 (s, 3H), 3.97 (s, 6H), 7.32 (s, 2H), 7.46-7.48 (m, 1H), 7.56-7.59 (m, 2H), 7.89 (d, *J* = 7.4 Hz, 2H), 8.70 (d, *J* = 1.8 Hz, 1H), 8.93 (d, *J* = 1.8 Hz, 1H), 13.93 (s, 1H); ¹³C NMR (150 MHz, DMSO-*d*₆): δ 56.5 (2C), 60.6, 104.7 (2C), 112.6, 127.8 (2C), 127.9, 128.4, 129.2, 129.6 (2C), 130.3, 138.2, 138.5, 143.7, 148.8, 152.9, 153.8 (2C). HRMS (ESI): calcd. for C₂₁H₁₉N₃NaO₃ [M+Na]⁺ 384.1319, found 384.1325.

4.1.4.2. 5-(*m*-Tolyl)-3-(3,4,5-trimethoxyphenyl)-1*H*-pyrazolo[3,4-*b*]pyridine (**13b**)

White solid, yield 67%, mp 158-160°C, ¹H NMR (600 MHz, DMSO-*d*₆): δ 2.41 (s, 3H), 3.74 (s, 3H), 3.91 (s, 6H), 7.23 (d, *J* = 7.4 Hz, 1H), 7.26 (s, 2H), 7.39-7.42 (m, 1H), 7.61 (d, *J* = 7.8 Hz, 1H), 7.65 (s, 1H), 8.62 (d, *J* = 2.0 Hz, 1H), 8.86 (d, *J* = 2.0 Hz, 1H), 13.87 (s, 1H); ¹³C NMR (150 MHz, DMSO-*d*₆): δ 21.6, 56.5 (2C), 60.6, 104.8 (2C), 112.6, 124.9, 128.2, 128.5, 128.6, 129.2, 129.4, 130.4, 138.2, 138.4, 138.8, 143.7, 148.9, 152.8, 153.8 (2C). HRMS (ESI): calcd. for C₂₂H₂₁N₃NaO₃ [M+Na]⁺ 398.1475, found 398.1481.

4.1.4.3. 5-(3-Methoxyphenyl)-3-(3,4,5-trimethoxyphenyl)-1*H*-pyrazolo[3,4-*b*]pyridine (**13c**)

White solid, yield 75%, mp 173-175°C, ¹H NMR (600 MHz, DMSO-*d*₆): δ 3.74 (s, 3H), 3.85 (s, 3H), 3.92 (s, 6H), 6.97-6.99 (m, 1H), 7.28 (s, 2H), 7.39-7.44 (m, 3H), 8.66 (d, *J* = 1.7 Hz, 1H), 8.89 (d, *J* = 1.7 Hz, 1H), 13.87 (s, 1H); ¹³C NMR (150 MHz, DMSO-*d*₆): δ 55.7, 56.5 (2C), 60.6, 104.7 (2C), 112.5, 113.2, 113.8, 120.1, 128.6, 129.2, 130.2, 130.6, 138.2, 140.0, 143.8, 148.9, 152.9, 153.8 (2C), 160.3. HRMS (ESI): calcd. for C₂₂H₂₂N₃O₄ [M+H]⁺ 392.1605, found 392.1624.

4.1.4.4. 5-(*p*-Tolyl)-3-(3,4,5-trimethoxyphenyl)-1*H*-pyrazolo[3,4-*b*]pyridine (**13d**)

White solid, yield 83%, mp 183-185°C, ¹H NMR (600 MHz, DMSO-*d*₆): δ 2.37 (s, 3H), 3.73 (s, 3H), 3.91 (s, 6H), 7.26 (s, 2H), 7.32 (d, *J* = 7.9 Hz, 2H), 7.72 (d, *J* = 7.9 Hz, 2H), 8.60 (d, *J* = 2.0 Hz, 1H), 8.85 (d, *J* = 2.0 Hz, 1H), 13.84 (s, 1H); ¹³C NMR (150 MHz, DMSO-*d*₆): δ 22.6, 56.5 (2C), 60.6, 104.7 (2C), 112.6, 127.7 (2C), 128.0, 129.2, 130.2 (2C), 130.3, 135.6, 137.3, 138.2, 143.6, 148.7, 152.8, 153.8 (2C). HRMS (ESI): calcd. for C₂₂H₂₂N₃O₃ [M+H]⁺ 376.1656, found 376.1655; C₂₂H₂₁N₃NaO₃ [M+Na]⁺ 398.1475, found 398.1476.

4.1.4.5. 5-(4-Fluorophenyl)-3-(3,4,5-trimethoxyphenyl)-1*H*-pyrazolo[3,4-*b*]pyridine (**13e**)

White solid, yield 75%, mp 218-219°C, ¹H NMR (600 MHz, DMSO-*d*₆): δ 3.74 (s, 3H), 3.91 (s, 6H), 7.27 (s, 2H), 7.34-7.37 (m, 2H), 7.88-7.90 (m, 2H), 8.64 (d, *J* = 1.5 Hz, 1H), 8.86 (d, *J* = 1.5 Hz, 1H), 13.87 (s, 1H); ¹³C NMR (150 MHz, DMSO-*d*₆): δ 56.5 (2C), 60.6, 104.8 (2C), 112.5, 116.3 (2C, d, *J* = 21.3 Hz), 128.4, 129.3, 129.9 (2C, d, *J* = 8.0 Hz), 130.1, 135.0 (d, *J* = 2.6 Hz), 138.2, 143.8, 148.8, 152.8, 153.8 (2C), 163.2 (d, *J* = 245.6 Hz). HRMS (ESI): calcd. for C₂₁H₁₉FN₃O₃ [M+H]⁺ 380.1405, found 380.1406; C₂₁H₁₈FN₃NaO₃ [M+Na]⁺ 402.1224, found 402.1229.

4.1.4.6. 5-(4-Chlorophenyl)-3-(3,4,5-trimethoxyphenyl)-1*H*-pyrazolo[3,4-*b*]pyridine (**13f**)

White solid, yield 64%, mp 220-221°C, ¹H NMR (600 MHz, DMSO-*d*₆): δ 3.74 (s, 3H), 3.91 (s, 6H), 7.27 (s, 2H), 7.57 (d, *J* = 8.5 Hz, 2H), 7.88 (d, *J* = 8.5 Hz, 2H), 8.67 (d, *J* = 2.0 Hz, 1H), 8.88 (d, *J* = 2.0 Hz, 1H), 13.90 (s, 1H); ¹³C NMR (150 MHz, DMSO-*d*₆): δ 56.5 (2C), 60.6, 104.8 (2C), 112.5, 128.6, 129.0, 129.1, 129.4 (2C), 129.6 (2C), 132.9, 137.4, 138.2, 143.8, 148.7, 152.9, 153.8 (2C). HRMS (ESI): calcd. for C₂₁H₁₉ClN₃O₃ [M+H]⁺ 396.1109, found 396.1105; C₂₁H₁₈ClN₃NaO₃ [M+Na]⁺ 418.0929, found 418.0926.

4.1.4.7. 5-(4-Bromophenyl)-3-(3,4,5-trimethoxyphenyl)-1*H*-pyrazolo[3,4-*b*]pyridine (**13g**)

White solid, yield 71%, mp 250-252°C, ¹H NMR (600 MHz, DMSO-*d*₆): δ 3.74 (s, 3H), 3.91 (s, 6H), 7.27 (s, 2H), 7.70 (d, *J* = 8.5 Hz, 2H), 7.81 (d, *J* = 8.5 Hz, 2H), 8.67 (d, *J* = 2.0 Hz, 1H), 8.87 (d, *J* = 2.0 Hz, 1H), 13.90 (s, 1H); ¹³C NMR (150 MHz, DMSO-*d*₆): δ 56.5 (2C), 60.6, 104.8 (2C), 112.5, 121.5, 129.1, 130.0 (2C), 130.1, 132.4 (2C), 137.7, 138.2, 143.9, 148.7, 152.9, 153.8 (2C). HRMS (ESI): calcd. for C₂₁H₁₈BrN₃NaO₃ [M+Na]⁺ 462.0424, found 462.0435.

4.1.4.8. 5-(4-Methoxyphenyl)-3-(3,4,5-trimethoxyphenyl)-1*H*-pyrazolo[3,4-*b*]pyridine (**13h**)

White solid, yield 70%, mp 199-201°C, ¹H NMR (600 MHz, DMSO-*d*₆): δ 3.73 (s, 3H), 3.82 (s, 3H), 3.91 (s, 6H), 7.08 (d, *J* = 8.7 Hz, 2H), 7.26 (s, 2H), 7.77 (d, *J* = 8.7 Hz, 2H), 8.57 (d, *J* = 1.3 Hz, 1H), 8.84 (d, *J* = 1.3 Hz, 1H), 13.82 (s, 1H); ¹³C NMR (150 MHz, DMSO-*d*₆): δ 55.7, 56.5 (2C), 60.6, 104.6 (2C), 112.6, 115.0, 127.6, 129.0 (2C), 129.2, 130.1, 130.8, 138.1, 143.5, 148.6, 152.6, 153.8 (2C), 159.4. HRMS (ESI): calcd. for C₂₂H₂₂N₃O₄ [M+H]⁺ 392.1605, found 392.1625; C₂₂H₂₁N₃NaO₄ [M+Na]⁺ 414.1424, found 414.1447.

4.1.4.9. 3-(3,4-dimethoxyphenyl)-5-(*p*-tolyl)-1*H*-pyrazolo[3,4-*b*]pyridine (**13i**)

White solid, yield 53%, mp 229-231°C, ¹H NMR (600 MHz, DMSO-*d*₆): δ 2.38 (s, 3H), 3.84 (s, 3H), 3.88 (s, 3H), 7.11 (d, *J* = 7.6 Hz, 1H), 7.33 (d, *J* = 7.8 Hz, 2H), 7.57 (s, 1H), 7.66 (d, *J* = 7.6

Hz, 1H), 7.73 (d, $J = 7.8$ Hz, 2H), 8.61 (s, 1H), 8.85 (s, 1H), 13.75 (s, 1H); ^{13}C NMR (150 MHz, DMSO- d_6): δ 21.2, 56.0, 56.1, 110.3, 112.5, 120.0, 126.4, 127.6 (3C), 127.9, 130.1 (3C), 135.6, 137.2, 143.5, 148.6, 149.5, 149.6, 152.8. HRMS (ESI): calcd. for $\text{C}_{21}\text{H}_{20}\text{N}_3\text{O}_2$ $[\text{M}+\text{H}]^+$ 346.1550, found 346.1559.

4.1.4.10. 3-(4-methoxyphenyl)-5-(*p*-tolyl)-1*H*-pyrazolo[3,4-*b*]pyridine (**13m**)

White solid, yield 50%, mp 197-199°C, ^1H NMR (600 MHz, DMSO- d_6): δ 2.38 (s, 3H), 3.84 (s, 3H), 7.11 (d, $J = 8.8$ Hz, 2H), 7.33 (d, $J = 7.9$ Hz, 2H), 7.74 (d, $J = 7.9$ Hz, 2H), 8.05 (d, $J = 8.8$ Hz, 2H), 8.63 (d, $J = 2.0$ Hz, 1H), 8.84 (d, $J = 2.0$ Hz, 1H), 13.74 (s, 1H); ^{13}C NMR (150 MHz, DMSO- d_6): δ 21.2, 55.7, 112.4, 114.9 (2C), 126.2, 127.6 (2C), 127.9, 128.5 (2C), 130.0, 130.1 (2C), 135.5, 137.2, 143.4, 148.5, 152.8, 159.7. HRMS (ESI): calcd. for $\text{C}_{20}\text{H}_{18}\text{N}_3\text{O}$ $[\text{M}+\text{H}]^+$ 316.1444, found 316.1458; $\text{C}_{20}\text{H}_{17}\text{N}_3\text{NaO}$ $[\text{M}+\text{Na}]^+$ 338.1264, found 338.1278.

4.2. Biology experiments

4.2.1. Antiproliferation assay *in vitro*

The antiproliferative activities *in vitro* of SMART and all the target compounds (**12a-m**, **13a-h** and **13l-m**) were tested by MTT assay followed the procedures as previous report.^[21]

4.2.2. Tubulin polymerization *in vitro*

The tubulin polymerization assay was performed by using the commercial tubulin polymerization assay kit (Cytoskeleton-Cat. #BK011P) referred to the protocol of manufacturer.

4.2.3. Immunofluorescence staining of tubulin

Immunofluorescence staining studies of SMART and compound **13d** were investigated using the reported method.^[22]

4.2.4. Cell cycle arrest

Cell cycle analysis assay was followed the procedure of relevant report.^[22]

4.3. Computational assay

4.3.1. DFT computation

Structural optimization of compounds **3-6** were performed at B3LYP/6-31G(d) level of Gaussian 09 software.^[23] The results of optimization showed the energy of two conformations for any molecule, and the unit a.u. of original energy value was converted into standard unit $\text{kJ}\cdot\text{mol}^{-1}$ (1 a.u. = $2625.50 \text{ kJ}\cdot\text{mol}^{-1}$). The results were listed in Table 1.

4.3.2. Molecular modeling

The molecular modeling studies were performed by using Accelrys Discovery Studio 3.0. The X-ray crystal structures of tubulin in complex with CA-4 (PDB: 5LYJ) was downloaded from the RCSB Protein Data Bank (<http://www.rcsb.org/structure/5LYJ>). The ligand **4**, **5**, and **13d** were energy-minimised with the CHARMM force-field and docked into colchicine binding site using CDOCKER protocol. The pictures in Figure 6 were edited with Discovery Studio 4.5 Visualizer.

Acknowledgements

We gratefully acknowledge the National Natural Science Foundation of China (81673293 and 81602969), Project funded by China Postdoctoral Science Foundation (215746), Plan for Development of Young Scholars of Shenyang Pharmaceutical University, National Natural Science Foundation of Liaoning (201602687), Doctoral Research Funding of Liaoning Province (201601144), Education Fund Item of Liaoning Province (201610163L12), and Liaoning Province Undergraduate Training Program for Innovation (201610163019, 201710163000202 and 201710163000094) for the generous financial support. This work was also supported by the Scientific and Technological Project of Henan Province (172102310102), Program for Innovative Research Team of the Ministry of Education and Program for Liaoning Innovative Research Team in University.

References

- [1] M.A. Jordan, L. Wilson, *Nat. Rev. Cancer* 4 (2004) 253-265.
- [2] C. Dumontet, M.A. Jordan, *Nat. Rev. Drug Discov.* 9 (2010) 790-803.
- [3] M.A. Jordan, K. Kamath, *Curr. Cancer Drug Tar.* 7 (2007) 730-742.
- [4] Y. Lu, J. Chen, M. Xiao, W. Li, D.D. Miller, *Pharm. Res.* 29 (2012) 2943-2971.
- [5] Y. Lu, C.-M. Li, Z. Wang, J. Chen, M.L. Mohler, W. Li, J.T. Dalton, D.D. Miller, *J. Med. Chem.* 54 (2011) 4678-4693.
- [6] Y. Lu, C.-M. Li, Z. Wang, C.R. Ross, II, J. Chen, J.T. Dalton, W. Li, D.D. Miller, *J. Med. Chem.* 52 (2009) 1701-1711.
- [7] M. Dong, F. Liu, H. Zhou, S. Zhai, B. Yan, *Molecules* 21 (2016) 1375-1400.
- [8] M. Zhai, L. Wang, S. Liu, L. Wang, P. Yan, J. Wang, J. Zhang, H. Guo, Q. Guan, K. Bao, Y. Wu, W. Zhang, *Eur. J. Med. Chem.* 156 (2018) 137-147.
- [9] C.-M. Li, Y. Lu, R. Narayanan, D.D. Miller, J.T. Dalton, *Drug Metab. Dispos.* 38 (2010) 2032-2039.
- [10] J. Sun, L. Chen, C. Liu, Z. Wang, D. Zuo, J. Pan, H. Qi, K. Bao, Y. Wu, W. Zhang, *Chem. Biol. Drug Des.* 86 (2015) 1541-1547.
- [11] Z. Wang, Q. Yang, Z. Bai, J. Sun, X. Jiang, H. Song, Y. Wu, W. Zhang, *Med. Chem. Commun.* 6 (2015) 971-976.

- [12] Q. Xu, H. Qi, M. Sun, D. Zuo, X. Jiang, Z. Wen, Z. Wang, Y. Wu, W. Zhang, *PLoS One* 10 (2015) e0128710.
- [13] L. Wang, K.W. Woods, Q. Li, K.J. Barr, R.W. McCroskey, S.M. Hannick, L. Gherke, R.B. Credo, Y. Hui, K. Marsh, R. Warner, J.Y. Li, N. Zielinski-Mozng, D. Frost, S.H. Rosenberg, H.L. Sham, *J. Med. Chem.* 45 (2002) 1697-1711.
- [14] G.C. Tron, F. Pagliai, E.D. Grosso, A.A. Genazzani, G. Sorba, *J. Med. Chem.* 48 (2005) 3260-3268.
- [15] J.P. Stasch, E.M. Becker, C. Alonso-Alija, H. Apeler, K. Dembowski, A. Feurer, R. Gerzer, T. Minuth, E. Perzborn, U. Pleiss, H. Schroder, W. Schroeder, E. Stahl, W. Steinke, A. Straub, M. Schramm, *Nature* 410 (2001), 212-215.
- [16] J. Witherington, V. Bordas, A. Gaiba, N.S. Garton, A. Naylor, A.D. Rawlings, B.P. Slingsby, D.G. Smith, A.K. Takle, R.W. Ward, *Bioorg. Med. Chem. Lett.* 13 (2003) 3055-3057.
- [17] J. Shen, D. Yang, Y. Liu, S. Qin, J. Zhang, J. Sun, C. Liu, C. Liu, X. Zhao, C. Chu, R. Liu, *Org. Lett.* 16 (2014) 350-353.
- [18] M.E. Kavanagh, A.G. Coyne, K.J. McLean, G.G. James, C.W. Levy, L.B. Marino, L.P.S. de Carvalho, D.S.H. Chan, S.A. Hudson, S. Surade, D. Leys, A.W. Munro, C. Abell, *J. Med. Chem.* 59 (2016) 3272-3302.
- [19] S. Lee, S.B. Park, *Org. Lett.* 11 (2009) 5214-5217.
- [20] M.S. Santos, A.M.R. Bernardino, L.C.S. Pinheiro, M.M. Canto-Cavalheiro, L.L. Leon, *J. Heterocyclic Chem.* 49 (2012) 1425-1428.
- [21] Q. Guan, C. Han, D. Zuo, M. Zhai, Z. Li, Q. Zhang, Y. Zhai, X. Jiang, K. Bao, Y. Wu, W. Zhang, *Eur. J. Med. Chem.* 87 (2014) 306-315.
- [22] D. Zuo, D. Guo, X. Jiang, Q. Guan, H. Qi, J. Xu, Z. Li, F. Yang, W. Zhang, Y. Wu, *Chemico-Biological Interact.* 227 (2015) 7-17.
- [23] M.J. Frisch, G.W. Trucks, H.B. Schlegel, G.E. Scuseria, M.A. Robb, J.R. Cheeseman, G. Scalmani, V. Barone, B. Mennucci, G.A. Petersson, H. Nakatsuji, M. Caricato, X. Li, H. P. Hratchian, A.F. Izmaylov, J. Bloino, G. Zheng, J.L. Sonnenberg, M. Hada, M. Ehara, K. Toyota, R. Fukuda, J. Hasegawa, M. Ishida, T. Nakajima, Y. Honda, O. Kitao, H. Nakai, T. Vreven, J.A. Montgomery, J.E.P. Jr., F. Ogliaro, M. Bearpark, J.J. Heyd, E. Brothers, K.N. Kudin, V.N. Staroverov, R. Kobayashi, J. Normand, K. Raghavachari, A. Rendell, J.C. Burant, S.S. Iyengar, J. Tomasi, M. Cossi, N. Rega, J.M. Millam, M. Klene, J.E. Knox, J.B. Cross, V. Bakken, C. Adamo, J. Jaramillo, R. Gomperts, R.E. Stratmann, O. Yazyev, A.J. Austin, R. Cammi, C. Pomelli, J.W. Ochterski, R.L. Martin, K. Morokuma, V.G. Zakrzewski, G.A. Voth, P. Salvador, J.J. Dannenberg, S. Dapprich, A.D. Daniels, Ö. Farkas, J.B. Foresman, J.V. Ortiz, J. Cioslowski, D.J. Fox, *Gaussian 09* (Gaussian, Inc., Wallingford CT, 2009).

Highlights

- Conformations of SMART analogues were analyzed based on DFT calculation.
- Target compounds were design rationally *via* ring tethering strategy.
- Most of the target compounds showed significant antiproliferative activities.
- Compound **13d** inhibited tubulin polymerization and caused cells arrest in G2/M phase.
- The binding mode of **13d** was determined by docking studies.